*Proceedings of the Twenty-sixth (2016) International Ocean and Polar Engineering Conference* **www.isope.org**
*Rhodes, Greece, June 26-July 1, 2016*

*ISBN 978-1-880653-88-3; ISSN 1098-6189*

# Detached-Eddy Simulation of Flows over a Circular Cylinder at High Reynolds Number

*Weiwen Zhao, Decheng Wan*, Ren Sun*

State Key Laboratory of Ocean Engineering, School of Naval Architecture, Ocean and Civil Engineering, Shanghai Jiao Tong University, Collaborative Innovation Center for Advanced Ship and Deep-Sea Exploration, Shanghai, China
*Corresponding author

## ABSTRACT

This paper presents a numerical study of flow over a circular cylinder at high Reynolds number using detached-eddy simulation (DES). The k-ω Shear Stress Transport (SST) based DES model is selected for handling massively separated flow. The computations are performed with an O-type grid and the instantaneous and statistical characteristics of the turbulent wake flow behind the cylinder is extensively studied. The results are compared with the available experimental data, as well as the previously published numerical data obtained from Reynolds-averaged Navier-Stokes (RANS) and large-eddy simulation (LES). The incompressible flow assumption and finite volume discretization is adopted. All the works are carried out with the use of OpenFOAM toolbox.

KEY WORDS: Circular cylinder; detached-eddy simulation; Shear Stress Transport; flow separation; high Reynolds number.

## INTRODUCTION

The Reynolds-Averaged Navier-Stokes (RANS) equations are widely used to model turbulence in industrial applications for its cheap costs. RANS do not mean to resolve any turbulent flow structures at any scale, but to model the time-averaged turbulent properties using varies kinds of mathematical formulations. All turbulent fluctuations are eliminated during the time averaging. Therefore, it is inaccurate to predict massively separated flows which contain detached eddies at different length scales. While the unsteady RANS (URANS) attempts to solve the problem but with little efforts. The large-eddy simulation (LES) and direct numerical simulation (DNS), on the other hand, is capable for accurately predicting unsteady flows since most turbulence eddies are resolved, but the cost is expensive mainly because the dense grid resolution at boundary layer and small time steps. Detached-eddy simulation (DES), as a hybrid RANS/LES method, combines the best part of the two worlds. The basic idea of DES is to model the attached flow near wall and to resolve the detached and free shear flows in the other regions. The original version of DES was proposed by Spalart et al. (1997). The version, referred as DES97 here, is a modification of the one-equation Spalart-Allmaras eddy viscosity model (Spalart and Allmaras, 1994). DES97 was soon discovered to be sensitive to wall-parallel grids in the boundary layers. It is caused by the simple and crude split of RANS and LES region. The improper arrangement of wall-parallel grids spacing results in the wrong regions for RANS and LES. The region in outer part of boundary layers which should be modeled by RANS turns to be resolved by LES. While the grid refinement is not enough to resolve all the eddy viscosities. A new version called delayed DES (DDES) was proposed by Spalart et al. (2006) to address that issue. Based on the basic idea of the hybrid model, Menter el al. (2003) also proposed the SST based DES model by modifying the two-equation SST model (Menter, 1994). The SST version of DES provides a "shield" which can prevent grid induced separation (GIS) and address model stress depletion (MSD).

The flow past a circular cylinder is a very complicated physical phenomenon, which involves boundary layer transition, flow separation, reattachment and/or vortex shedding. It has been studied for over half a century both experimentally and numerically, while it is still very difficult to reveal the essence of natural behind the phenomenon. Flow around a cylinder at subcritical Reynolds number (Re=3900) was extensively studied numerically. It has become a benchmarking case for LES (Beaudan and Moin, 1994; Mittal and Moin, 1997; Kravchenko and Moin, 2000). Ma et al. (2000) performed DNS studies for cylinder flow at Re=3900. Good agreements for mean streamwise velocity and power spectra are obtained at both near wake and far downstream compared with the experimental data. Besides LES and DNS, Zhao et al. (2012) detailedly studied DES simulation of cylinder flows at Re=3900. The influence of spanwise lengths, grid resolutions and numerical schemes are discussed. There are also some publications of cylinder flow at relevant high Reynolds number. Breuer (2000) investigated the cylinder flow at Re=140,000 in order to evaluate the applicability of LES for practically relevant high Reynolds number flows. The LES results of mean flow field, resolved Reynolds stresses and integral parameters agreed fairly well with the experimental data. In addition, Travin et al. (2000) carried out DES simulations for cylinder at Re=50,000, 140,000 and $3\times10^6$, but only met with partial success. However, both studies of Breuer and Travin et al. failed on grid convergence study (i.e. the finest grid doesn't lead to best results compared to experimental data).

This paper takes the challenge of applying SST based DES model to high Reynolds number (Re=140,000) cylinder flow. Several results, including mean velocity profile, pressure distribution and integral parameters, are presented and analyzed. The main objective of the present paper is to help building confidence of DES for massively separated flows at high Reynolds number.

## TURBULENCE MODELING

### Menter's SST Model

The version of Menter's SST model implemented in the official OpenFOAM is a modified version (Menter and Esch, 2001; Menter et al., 2003) rather than the original version (Menter, 1994). The modification is replacing the vorticity by the invariant measure of the strain rate. The notations in the following paragraphs take the definition in OpenFOAM as standard.

The k- and ω-equation are given by

$$\frac{\partial k}{\partial t}+\frac{\partial (u_j k)}{\partial x_j}=\tilde{G}-\beta^* k\omega+\frac{\partial}{\partial x_j}\left[(\nu+\alpha_k \nu_t)\frac{\partial k}{\partial x_j}\right] \tag{1}$$

$$\frac{\partial \omega}{\partial t}+\frac{\partial (u_j \omega)}{\partial x_j}=\gamma S^2-\beta\omega^2+\frac{\partial}{\partial x_j}\left[(\nu+\alpha_\omega \nu_t)\frac{\partial \omega}{\partial x_j}\right]+(1-F_1)CD_{k\omega} \tag{2}$$

where, $\tilde{G}=\min\left(G, c_1\beta^* k\omega\right)$ and $G=\nu_t S^2$. $F_1$ is a blending function which is defined as

$$F_1=\tanh\left(\arg_1^4\right),\quad \arg_1=\min\left[\max\left(\frac{\sqrt{k}}{\beta^*\omega y},\frac{500\nu}{y^2\omega}\right),\frac{4\alpha_{\omega 2}k}{CD_{k\omega}^* y^2}\right] \tag{3}$$

where, $CD_{k\omega}^*=\max\left(CD_{k\omega}, 10^{-10}\right)$ and $CD_{k\omega}=2\alpha_{\omega 2}\frac{1}{\omega}\frac{\partial k}{\partial x_j}\frac{\partial \omega}{\partial x_j}$. All the constants in transport equations are obtained through blending function

$$\phi=F_1\phi_1+(1-F_1)\phi_2 \tag{4}$$

in which $\phi$ represents $\alpha$, $\beta$ and $\gamma$ in the k- and ω-equation.

The eddy viscosity is given by

$$\nu_t=\frac{a_1 k}{\max(a_1\omega, b_1 S F_2)} \tag{5}$$

where $S$ is the strain rate defined as $S=\sqrt{2S_{ij}S_{ij}}$, and $S_{ij}=\frac{1}{2}\left(\frac{\partial u_i}{\partial x_j}+\frac{\partial u_j}{\partial x_i}\right)$. $F_2$ is another blending function defined as

$$F_2=\tanh\left(\arg_2^2\right),\quad \arg_2=\max\left(2\frac{\sqrt{k}}{\beta^*\omega y},\frac{500\nu}{y^2\omega}\right) \tag{6}$$

All constants used in this paper are the same with reference (Menter et al., 2003).

### DES Modification

Menter et al. (2003) modified the k-equation by adding a production coefficient $F_{DES}$ to the dissipation term

$$\frac{\partial k}{\partial t}+\frac{\partial (u_j k)}{\partial x_j}=\tilde{G}-\beta^* k\omega F_{DES}+\frac{\partial}{\partial x_j}\left[(\nu+\alpha_k \nu_t)\frac{\partial k}{\partial x_j}\right] \tag{7}$$

in which $F_{DES}$ is defined as

$$F_{DES}=\max\left(\frac{L_t}{C_{DES}\Delta}(1-F_S),1\right) \tag{8}$$

where, $L_t=\sqrt{k}/\left(\beta^*\omega\right)$ is the computed turbulent length scale, $\Delta=\sqrt[3]{\Delta x\Delta y\Delta z}$ is grid size, $C_{DES}$ is the DES constant which is 0.61 herein. $F_S$ can be $F_1$ or $F_2$, and $F_2$ is used in this paper.

## NUMERICAL OVERVIEW

The numerical simulation presented here is an extend work of the previous studied cylinder flow at low (sub-critical) Reynolds number *Re*=3900. This paper focused on the high Reynolds number flow *Re*=140,000. Although it is subcritical under this Reynolds number, i.e., the separated boundary layer remains laminar while transitions take place along the free shear layers, the flows are forced to be supercritical through the use of RANS close to the wall.

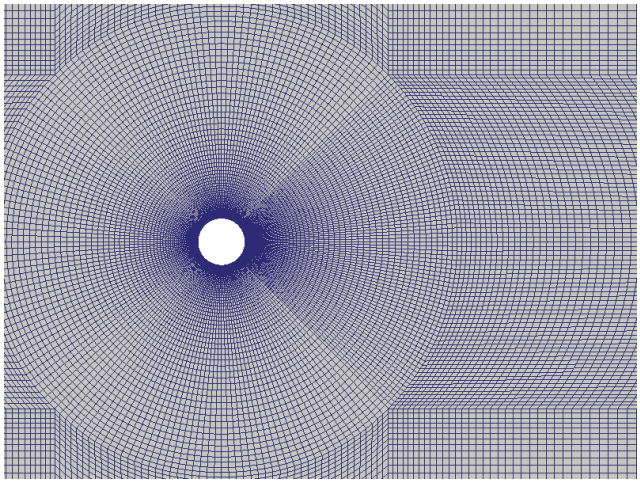

Fig. 1. Computational mesh

The computations utilize a O-type grid in the center of computational domain, which extends to $15D<x<30D$ and $-15D<y<15D$. The total number of cells on the *x*-*y* plane is 40,500. A 10*D* diameter O-type grid with a grid points of 231×101 is adopted in the vicinity of the circular cylinder. The downstream circumference is refined to capture more detailed flow characteristics, see Fig. 1. Grid points for the remaining blocks are: upstream block 51×31, wake block 81×81, side blocks from inlet to outlet 31×31, 51×31 and 81×31. The first layer height is 0.0002*D*, corresponding to approximately $y^+$=2. Two different spanwise lengths, $\pi D$ and $2\pi D$, are selected for numerical investigation.

The grid resolution for spanwise direction is also investigated. As indicated by Travin et al. (2000) and Breuer (2000), grid is not convergent on DES and LES simulations, i.e., the finest grid didn't get the best agreement for all quantities compared with experiments.

The simulations in this work are performed using the single-phase incompressible Navier-Stokes solver *pimpleFoam*, which is a standard solver provided by OpenFOAM, with a newly implemented SST-DES turbulence model. The second order implicit Euler scheme is used for temporal discretization. A second order Gauss integration is used for spatial gradient calculations. The convection operator is discretized using a total variation diminishing (TVD) scheme. For all computations shown in this paper, a non-dimensional time step $\Delta t \cdot U_\infty / D$ =0.0056 is selected, where $D$ is the diameter of cylinder and $U_\infty$ is the free stream velocity.

Table 1. Summary of cylinder flow test cases

| Case | $Re$ | $L_z$ | $N_z$ | $C_d$ | $C_l'$ | $St$ | $-C_{pb}$ | $\theta_{sep}$ | $L_{rec}/D$ |
|---|---|---|---|---|---|---|---|---|---|
| A | $1.4\times10^5$ | $\pi D$ | 32 | 0.71 | 0.07 | 0.25 | 0.71 | 93.3 | 1.57 |
| B | $1.4\times10^5$ | $\pi D$ | 64 | 0.71 | 0.06 | 0.27 | 0.71 | 93.6 | 1.48 |
| C | $1.4\times10^5$ | $2\pi D$ | 64 | 0.72 | 0.07 | 0.25 | 0.73 | 94.0 | 1.41 |
| Travin et al. | $1.4\times10^5$ | $2D$ | 30/42 | 0.57-0.65 | 0.06-0.10 | 0.28-0.31 | 0.65-0.7 | 93°-99° | 1.1-1.4 |
| Hansen et al. | $1.4\times10^5$ | $4D$ | 30 | 0.59 | - | 0.29 | 0.72 | - | - |
| Lo et al. | $1.4\times10^5$ | $1D/2D$ | 40 | 0.62-0.70 | - | 0.287-0.305 | 0.75-0.914 | 100°-105° | 0.60-0.81 |
| Roshko | $8.4\times10^6$ | - | - | 0.62-0.74 | - | 0.27 | - | - | - |

The results of case A and B agree fairly well with slightly different Strouhal number, indicating that grid resolution along the spanwise direction is not a critical influence factor for cylinder flows.

The drag and lift coefficient as well as other quantities discrepancies are negligible for case A and C, suggesting that the aspect ratio $L/D$ of the circular cylinder has little influence on the results, which is different with the conclusion of Breuer (2000).

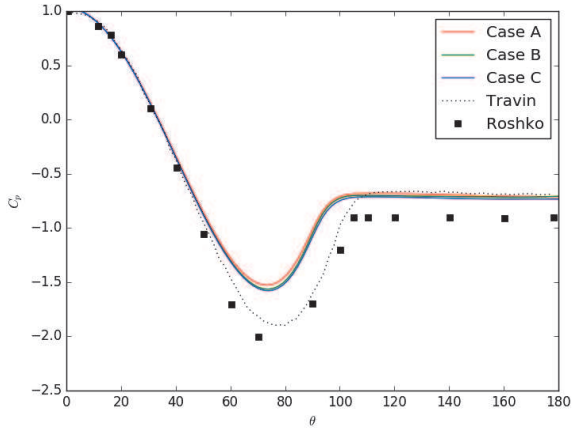


Fig. 2. Mean pressure coefficient around the cylinder surface

Fig. 2 shows the mean pressure coefficient distribution around the cylinder surface. The result of Travin et al (2000) is TS1 at Reynolds number $Re = 1.4\times10^5$ with a forced turbulent separation regime. The experimental data of Roshko (1961) is at supercritical Reynolds number $Re = 8.4\times10^6$. The pressure around the cylinder surface predicted by case A, B and C are slightly different, indicating the spanwise grid resolution and length have little effect on the pressure distribution on cylinder surface. However, comparing with Travin's results, although the base pressure coefficient agrees fairly well, the pressure distribution at $\theta = 50^\circ \sim 110^\circ$ differs a lot. A possible explanation is the different turbulence level at the inlet boundary condition. Travin applied SA-DES and the free-stream turbulence level are given by set the eddy viscosity $\tilde{\nu}$ 5 times the molecular viscosity. While in the current study which employs SST-DES as the turbulence closure, the free-stream turbulence level is specified by $k$ and $\omega$ at the inlet boundary condition.

## RESULTS AND DISCUSSION

Table 1 shows the case setup and averaged quantities of the current simulations: the spanwise length $L_z$, grid resolution on spanwise direction $N_z$, drag coefficient $C_d$, root mean square (RMS) lift coefficient $C_l'$, Strouhal number $St$, base pressure coefficient $C_{pb}$, separation angle $\theta_{sep}$, and non-dimensional recirculation zone length $L_{rec}/D$. The averaging time for these quantities are about 35 shedding cycles. For comparison, the predicted results of Travin et al. (2000), Hansen and Forsythe (2003), Lo et al. (2005), the experiment measurement of Roshko (1961) are also included. It should be noticed that all results presented here are turbulent separation cases.

Fig. 3 is the non-dimensional mean stream-wise velocity contours $u/U_\infty$ from -0.3 to 1.5 with an interval of 0.1. From top to bottom, corresponding to case A, B and C. The slightly differences among the three are the recirculation bubbles. Spanwise grid resolution will influent the length of recirculation zone. It seems refine grid at spanwise direction could partially improve results. While the results of A and C indicating that increasing spanwise length may also get better results. Regarding the influence of spanwise grid resolution and length, more systematic spanwise grid resolution investigation should be carried out to prove the hypothesis.

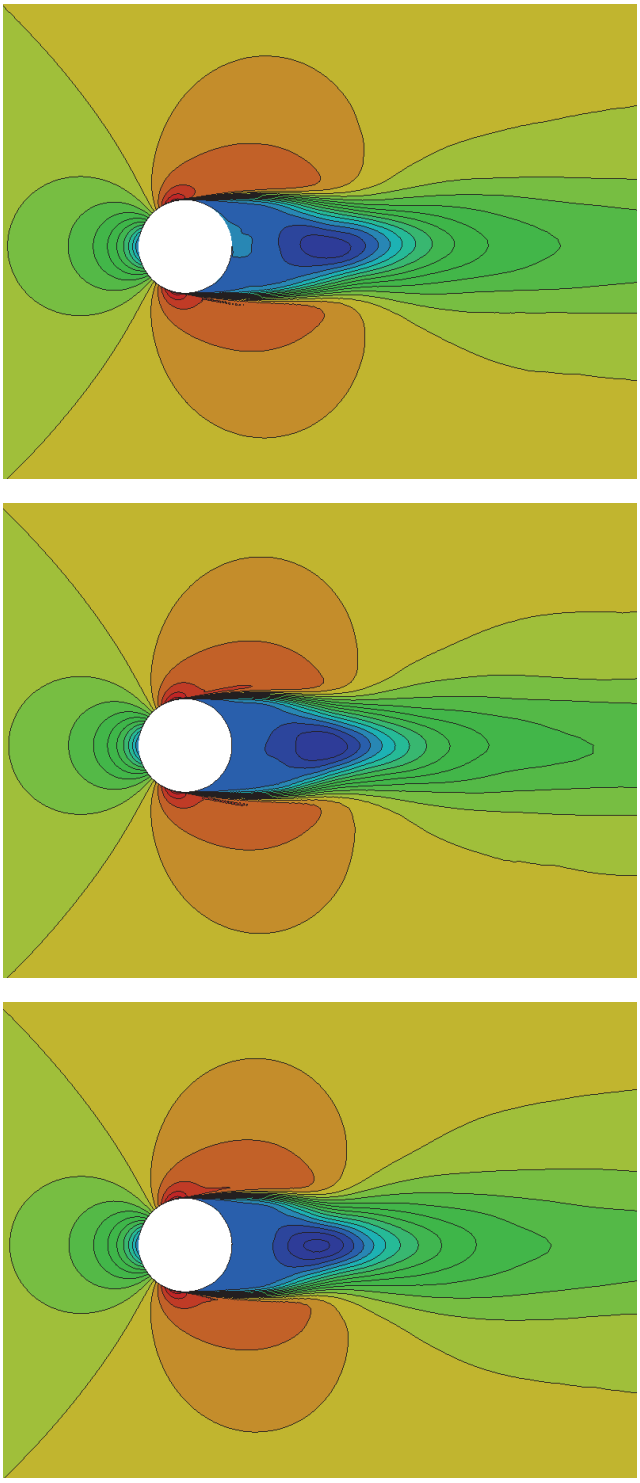

Fig. 3. Mean stream-wise velocity contours: upper – A, middle – B, lower – C

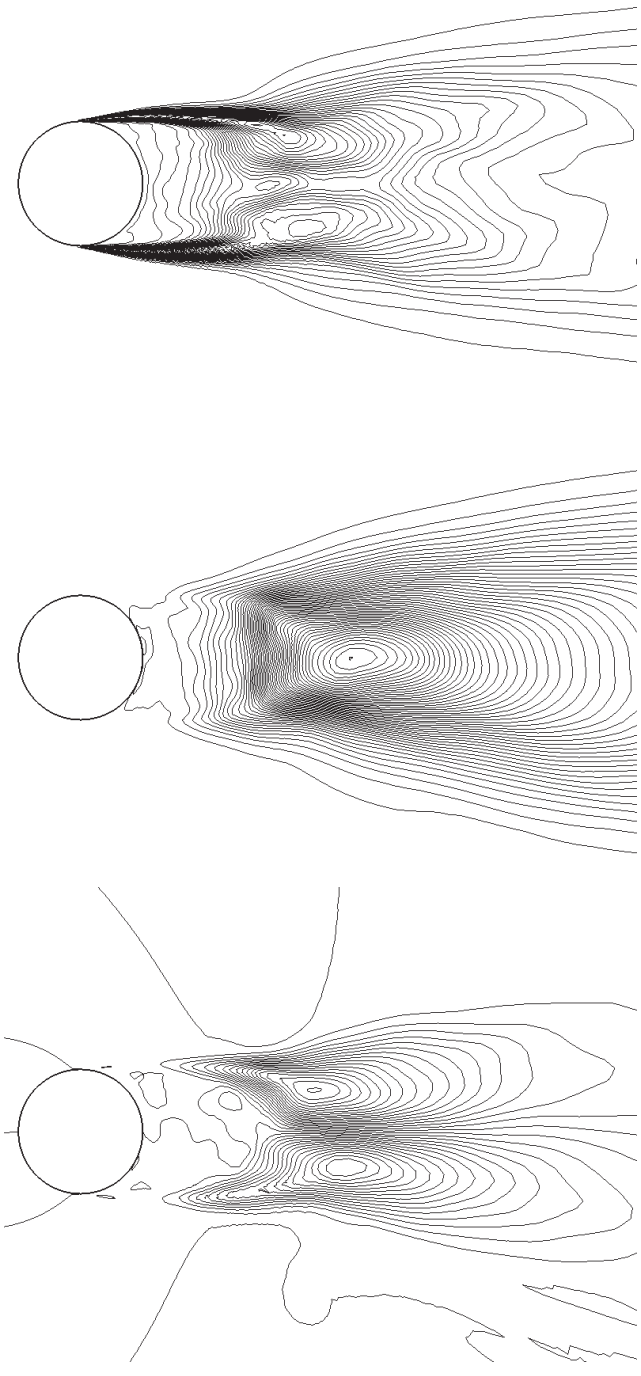

Fig. 4. Reynolds stress contours for case B: upper - $\overline{u'u'}$ , middle - $\overline{v'v'}$ , lower - $\overline{u'v'}$

Fig. 4 is the Reynolds stress contours with the same interval 0.01. It is very interesting that these patterns are similar to the results of Travin et al. (2000) despite the different separation regime, i.e. the results given

by Travin et al (2000) are at laminar separation regime, while the present study is at turbulent separation. This shows the flow separation regime have little influence on the Reynolds stress patterns in the cylinder wake.

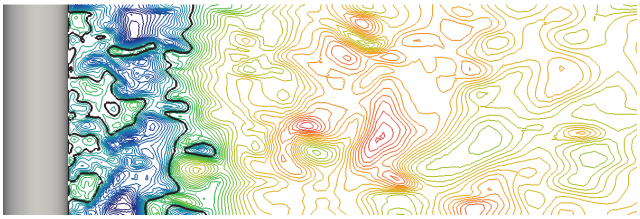

Fig. 5. Instantaneous streamwise velocity profile in $y$=0 plane in the wake of cylinder (case B)

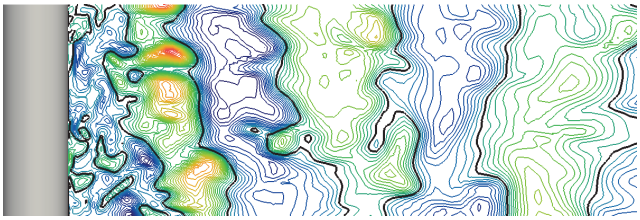

Fig. 6. Instantaneous cross-flow velocity profile in $y$=0 plane in the wake of cylinder (case B)

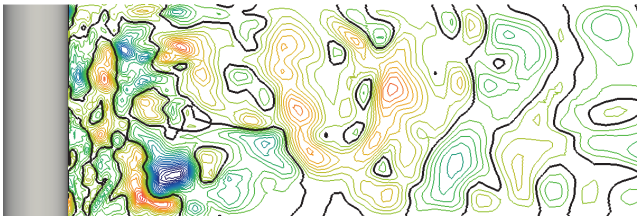

Fig. 7. Instantaneous spanwise velocity profile in $y$=0 plane in the wake of cylinder (case B)

Figs. 5-7 show the instantaneous streamwise, cross-flow and spanwise velocity profile in the wake of the circular cylinder, respectively. The three figures are contoured by the same level, i.e. 60 contours of non-dimensional (by free stream velocity) velocity component from -1.5 to 1.5. The black thick lines represent the zero value of the contours. The recirculation bubble and Kaman vortex street are clearly seen in Fig. 4 and Fig. 6, respectively. In addition, the strong three dimensional effects along spanwise direction are also observed.

Fig. 8 illustrates the contours of SGS eddy viscosity of three planes. The visualization shows clearly 2D Karman vortex street patterns in each plane. The slight difference vortex street pattern among each plane indicating the three dimensional turbulent structures, which can also be observed in Fig. 9, along the spanwise direction.

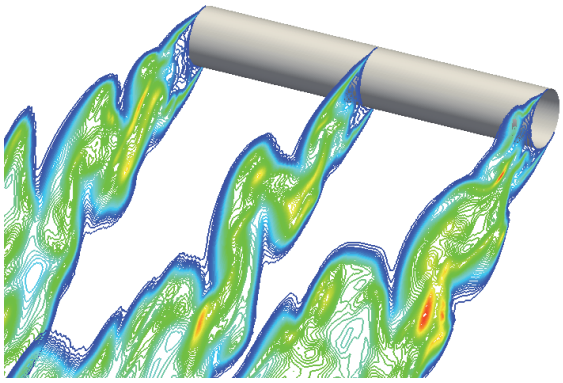

Fig. 8. Instantaneous SGS viscosity contours (case C)

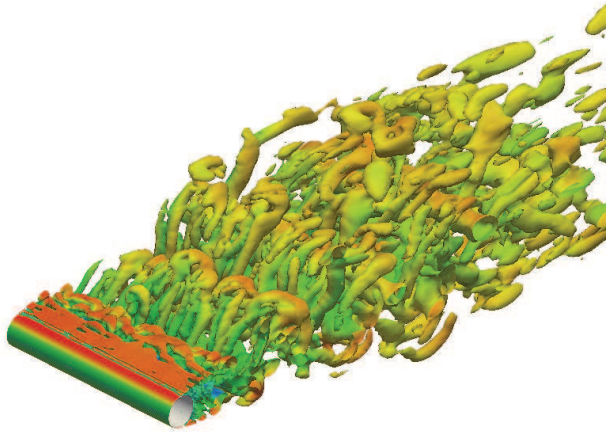

Fig. 9. Instantaneous vorticity contoured by $Q$=10, $Q = 0.5(|\Omega|^2 - |S|^2)$

## CONCLUSIONS

Flow past a circular cylinder at $Re$ =140,000 is studied. Although it is subcritical at this Reynolds number, the numerical simulations are forced to be supercritical and flow separates in turbulent regime. The SST base DES turbulence model is utilized for simulation. Different spanwise length and grid resolutions are investigated. For SST-DES simulations of cylinder flow, most averaged quantities are not sensitive to spanwise resolution and length. The magnitude of predicted pressure distributions along cylinder surface are smaller than Travin's result. Reasons yet unknown to the author. High Reynolds number flows are still challenging for DES and more systematic tests will need to be carried out. Future tests may assess the influence of time step, grid size, numerical schemes, and the most important, laminar separation regime at this Reynolds number.

## ACKNOWLEDGEMENTS

This work is supported by the National Natural Science Foundation of China (51379125, 51490675, 11432009, 51579145, 11272120), Chang Jiang Scholars Program (T2014099), Program for Professor of Special Appointment (Eastern Scholar) at Shanghai Institutions of Higher Learning (2013022), Innovative Special Project of Numerical Tank of Ministry of Industry and Information Technology of China (2016-23) and Foundation of State Ley Laboratory of Ocean Engineering (GKZD010065), to which the authors are most grateful.

## REFERENCES

Beaudan, P, and Moin, P (1994). "Numerical experiments on the flow past a circular cylinder at sub-critical Reynolds number," Stanford University.

Breuer, M (2000). "A challenging test case for large eddy simulation: high Reynolds number circular cylinder flow," *Int J Heat Fluid Flow*, 21(5), 648–654.

Hansen, RP, and Forsythe, JR (2003). "Large and detached eddy simulations of flow over a circular cylinder using unstructured grids," *41 St Aerosp Sci Meet Exhib AIAA*, 775.

Kravchenko, AG, and Moin, P (2000). "Numerical studies of flow over a circular cylinder at ReD=3900," *Phys Fluids*, 12(2), 403–417.

Lo, S-C, Hoffmann, KA, and Dietiker, J-F (2005). "Numerical investigation of high reynolds number flows over square and circular cylinders," *J Thermophys Heat Transf*, 19(1), 72–80.

Ma, X, Karamanos, G-S, and Karniadakis, GE (2000). "Dynamics and low-dimensionality of a turbulent near wake," *J Fluid Mech*, 410, 29–65.

Menter, FR (1994). "Two-equation eddy-viscosity turbulence models for engineering applications," *AIAA J*, 32(8), 1598–1605.

Menter, F, and Esch, T (2001). "Elements of industrial heat transfer predictions," *16th Braz Congr Mech Eng COBEM*, Uberlandia, Brazil, 26–30.

Menter, FR, Kuntz, M, and Langtry, R (2003). "Ten years of industrial experience with the SST turbulence model," *Turbul Heat Mass Transf*, 4(1), 625–632.

Mittal, R, and Moin, P (1997). "Suitability of Upwind-Biased Finite Difference Schemes for Large-Eddy Simulation of Turbulent Flows," *AIAA J*, 35(8), 1415–1417.

Roshko, A (1961). "Experiments on the flow past a circular cylinder at very high Reynolds number," *J Fluid Mech*, 10(03), 345–356.

Spalart, PR, and Allmaras, SR (1994). "A one-equation turbulence model for aerodynamic flows," *Rech Aerosp*, 1, 5–21.

Spalart, P, Jou, W, Strelets, M, and Allmaras, S (1997). "Comments on the feasibility of LES for wings, and on a hybrid RANS/LES approach," *Adv DNSLES*, 1, 4–8.

Spalart, PR, Deck, S, Shur, ML, Squires, KD, Strelets, MK, and Travin, A (2006). "A new version of detached-eddy simulation, resistant to ambiguous grid densities," *Theor Comput Fluid Dyn*, 20(3), 181–195.

Travin, A, Shur, M, Strelets, M, and Spalart, P (2000). "Detached-Eddy Simulations Past a Circular Cylinder," *Flow Turbul Combust*, 63(1-4), 293–313.

Zhao, R, Liu, J, and Yan, C (2012). "Detailed Investigation of Detached-Eddy Simulation for the Flow Past a Circular Cylinder at Re=3900," *Progress in Hybrid RANS-LES Modelling*, Springer Berlin Heidelberg, 401–412.